HHS Public Access

Author manuscript

J Neurochem. Author manuscript; available in PMC 2015 December 09.

Published in final edited form as:

J Neurochem. 2014 July ; 130(1): 75–86. doi:10.1111/jnc.12709.

Stable over-expression of the 2-oxoglutarate carrier enhances neuronal cell resistance to oxidative stress via Bcl-2-dependent mitochondrial GSH transport

Heather M. Wilkins[*], **Samantha Brock**[*], **Josie J. Gray**[*], and **Daniel A. Linseman**[*,†,‡]

[*]Department of Biological Sciences and Eleanor Roosevelt Institute, University of Denver, Denver, Colorado, USA

[†]Research Service, Veterans Affairs Medical Center, Denver, Colorado, USA

[‡]Division of Clinical Pharmacology and Toxicology, Department of Medicine and Neuroscience Program, University of Colorado Denver, Aurora, Colorado, USA

Abstract

Mitochondrial glutathione (GSH) is a key endogenous antioxidant and its maintenance is critical for cell survival. Here, we generated stable NSC34 motor neuron-like cell lines over-expressing the mitochondrial GSH transporter, the 2-oxoglutarate carrier (OGC), to further elucidate the importance of mitochondrial GSH transport in determining neuronal resistance to oxidative stress. Two stable OGC cell lines displayed specific increases in mitochondrial GSH content and resistance to oxidative and nitrosative stressors, but not staurosporine. Inhibition of transport through OGC reduced levels of mitochondrial GSH and resensitized the stable cell lines to oxidative stress. The stable OGC cell lines displayed significant up-regulation of the anti-apoptotic protein, B cell lymphoma 2 (Bcl-2). This result was reproduced in parental NSC34 cells by chronic treatment with GSH monoethylester, which specifically increased mitochondrial GSH levels. Knockdown of Bcl-2 expression decreased mitochondrial GSH and resensitized the stable OGC cells to oxidative stress. Finally, endogenous OGC was co-immunoprecipitated with Bcl-2 from rat brain lysates in a GSH-dependent manner. These data are the first to show that increased mitochondrial GSH transport is sufficient to enhance neuronal resistance to oxidative stress. Moreover, sustained and specific enhancement of mitochondrial GSH leads to increased Bcl-2 expression, a required mechanism for the maintenance of increased mitochondrial GSH levels.

Keywords

2-oxoglutarate carrier; Bcl-2; glutathione; mitochondria; nitrosative stress; oxidative stress

Oxidative stress, particularly at the level of the mitochondria, and mitochondrial dysfunction play key roles in the pathogenesis underlying several neurodegenerative diseases (Lin and

Address correspondence and reprint requests to Dr Daniel Linseman, Department of Biological Sciences and Eleanor Roosevelt Institute, University of Denver, 2199 S. University Blvd., Denver, CO 80208, USA. daniel.linseman@du.edu.

Conflict of interest disclosure

All experiments were conducted in compliance with the ARRIVE guidelines. The authors have no conflict of interest to declare.

Beal 2006). While the CNS accounts for a mere two percent of total body weight, it generates approximately 20% of the resting metabolic rate (Silver and Erecinska 1998). Furthermore, neurons require high amounts of ATP production, most of which is generated from oxidative phosphorylation at the level of the mitochondrial electron transport chain, and are thus particularly vulnerable to reactive oxygen species generated by electron leakage from the electron transport chain (Kann and Kovács 2007). If reactive oxygen species production is not balanced by free radical scavenging systems, such as glutathione (GSH) or thioredoxin, then mitochondrial oxidative stress occurs triggering damage to DNA, lipids, and proteins, ultimately leading to apoptotic or necrotic degeneration of neurons (Lin and Beal 2006).

GSH, an endogenous tripeptide antioxidant, is the most prominent cellular thiol and is present at concentrations which are 500–1000 times greater than other free radical scavenging systems (Schafer and Buettner 2001; Filomeni *et al.* 2002). There are several reservoirs of GSH throughout the cell, but in particular the mitochondrial GSH pool has been shown to be critical for cell survival in several different systems (Meredith and Reed 1982, 1983; Muyderman *et al.* 2007; Wilkins *et al.* 2013). GSH is compartmentalized into mitochondria via a facilitated transport process involving inner mitochondrial membrane anion transporters such as the dicarboxylate (*Slc25a10*; DIC), 2-oxoglutarate (*Slc25a11*; OGC), and tricarboxylate (*Slc25a1*; TCC) carriers (Lash 2006; Wadey *et al.* 2009; Kamga *et al.* 2010). We have previously shown that mitochondrial GSH transport is critical for cell survival in primary cerebellar granule neurons; discrete inhibition or molecular knockdown of a single mitochondrial GSH transporter (DIC) significantly sensitized these neurons to both oxidative and nitrosative stress (Wilkins *et al.* 2013). These previous findings indicate that not only is the mitochondrial GSH pool critical, but that mitochondrial GSH transport is a major determinant of neuronal susceptibility to oxidative stress.

To further elucidate the importance of mitochondrial GSH transport on neuronal viability, we derived NSC34 motor neuron-like cell lines that stably over-express V5-tagged OGC. Here, we show that the stable OGC cell lines display a specific increase in mitochondrial GSH levels. In addition, these OGC stable cell lines are significantly resistant to oxidative and nitrosative stress, as well as to a GSH depleting agent, ethacrynic acid, but not to a classically Bax-dependent apoptotic inducer, staurosporine. Furthermore, the stable OGC cell lines showed a significant up-regulation of B cell lymphoma 2 (Bcl-2) protein expression, an effect that is dependent on enhanced mitochondrial GSH levels. Finally, either chemical inhibition of OGC transport function or knockdown of Bcl-2 using siRNA led to a decrease in mitochondrial GSH levels and resensitization of the stable OGC cell lines to oxidative stress. It has been previously shown in several systems using either recombinant proteins or transient transfection that Bcl-2 and OGC can interact in a GSH-dependent manner (Gallo *et al.* 2011; Wilkins *et al.* 2012). However, here we provide the first evidence that endogenous Bcl-2 and OGC interact in a GSH-dependent manner in lysates derived from rat brain. Overall, these findings suggest a synergistic mechanism between Bcl-2 and OGC in facilitating mitochondrial GSH transport and further establish the importance of mitochondrial GSH transport in sustaining neuronal viability under conditions of increased oxidative and nitrosative stress.

Methods

Materials

Phenylsuccinic acid, L-reduced glutathione, ethacrynic acid, staurosporine, primary antibody against α-tubulin, and GSH monoethylester were purchased from Sigma-Aldrich (St. Louis, MO, USA). The 3-(4,5-dimethylthiazol-2-yl)-2,5-diphenyltetrazolium bromide (MTT) cell viability assay, Geneticin (G418) and Lipofectamine were obtained from Invitrogen (Carlsbad, CA, USA). The GSH assay was purchased from Oxford Biomedical (Rochester Hills, MI, USA). The mitochondrial/cytosolic fractionation kit was from Biovision (Mountain View, CA, USA). Antibodies against cytochrome *c* oxidase IV (Cox-IV) and γ-glutamylcysteine ligase (GCL) catalytic subunit were purchased from Cell Signaling (Beverly, MA, USA). Anti-glyceraldehyde 3-phosphate dehydrogenase (Anti-GAPDH), anti-Bcl-2, anti-OGC, non-immune IgG, anti-neuron-specific β3 tubulin, and anti-V5 antibodies were purchased from Abcam (Cambridge, MA, USA). Sodium nitroprusside was purchased from Calbiochem (Billerica, MA, USA). Secondary antibodies for immunoblotting and reagents for enhanced chemiluminescence were obtained from GE Life Sciences (Piscataway, NJ, USA). DharmaFECT Transfection Kit, smart pool siRNA against mouse Bcl-2, and non-target siRNA were purchased from Thermoscientific Pierce Biotechnology (Rockford, IL, USA). Optimem and Dulbecco's modified Eagle's medium were obtained from Gibco (Carlsbad, CA, USA). V5-OGC plasmid was a generous gift from Dr Larry Lash (Wayne State University). NSC34 cells were kindly provided by Dr Neil Cashman (University of British Columbia).

Establishment of stable OGC NSC34 cell lines

NSC34 cells were plated at 80% confluence in 10-cm cell culture dishes, and transfected with 40 μg of V5-OGC plasmid DNA using a standard Lipofectamine 2000 protocol. At 24 h post transfection cells were split into two cell culture dishes and the following day 500 μg/mL of G418 was added to the media to allow for the selection of transfected cells. Media were changed every 3 days with the addition of 500 μg/mL of G418. Clones were then selected and grown in a 24-well plate in duplicate, grown to confluence and immunoblotted for V5 expression. High expressing clones were propagated for further experiments.

Cell culture of parental wild-type and stable OGC NSC34 cell lines

NSC34 wild-type (WT) cultures were grown in Dulbecco's modified Eagle's medium high-glucose medium containing 10% heat-inactivated fetal bovine serum, 2 mM L-glutamine, and 100 units/mL/100 μg/mL penicillin/streptomycin. NSC34 stable OGC cell lines were grown in identical media containing 500 μg/mL of G418. Cells were plated on 6-well plates and grown to ~ 80% confluence at 37°C in 10% CO_2, at which time cells were utilized for the described experiments.

Mitochondrial/cytosolic fractionation

Cells were treated as indicated in the Figure Legends or Results section. Media were aspirated and cells were washed once with 1X ice-cold phosphate-buffered saline (PBS), pH 7.4. One ml of cytosolic buffer provided in the kit was diluted 1 : 5 in ddH_2O, with added

protease inhibitor cocktail and 1 mM dithiothreitol as per the manufacturer's recommendations. A 100-μL aliquot of the cytosolic buffer was added per well and incubated on ice for 20 min, at which point cells were harvested and homogenized with 40 passes of a Dounce homogenizer. Samples were then spun down at 720 g for 10 min at 4°C. The supernatant was transferred to a new tube which was labeled 'mitochondrial fraction' and the supernatant was spun down at 10 000 *g* for 30 min at 4°C. The supernatant was transferred to a new tube which was labeled the 'cytosolic fraction' and the pellet in the mitochondrial fraction tube was resuspended in 100 μL of mitochondrial buffer (provided in the kit) with protease inhibitor cocktail and 1 mM dithiothreitol as per the manufacturer's recommendations. Samples were immediately used for further experiments.

Glutathione assay

Total glutathione [reduced GSH+oxidized glutathione (GSSG)] was measured using an assay kit (DTNB) from Oxford Biomedical, following the manufacturer's protocol. All glutathione measurements were normalized to protein concentration.

Immunoblot analysis

Protein concentrations of samples were determined by a bicinchoninic acid protein assay. Equal protein concentrations were subjected to sodium dodecyl sulfate–polyacrylamide gel electrophoresis, transferred, and immunoblotted as described previously (Linseman *et al.* 2001). Briefly, polyvinylidene difluoride membranes were incubated in blocking solution (10% bovine serum albumin and 0.01% sodium azide diluted in PBS with 0.1% Tween 20; PBS-T) for 1 h at ~25°C. The primary antibodies were diluted in blocking solution at the manufacturer's recommended dilution and membranes were either incubated with primary antibody for 1 h at ~25°C or overnight at 4°C, as per manufacturer's recommendations. Membranes were then washed 5× over 30 min with PBS-T. Next, membranes were incubated for 1 h at ~25°C with horseradish peroxidase-conjugated secondary antibodies that were diluted to appropriate concentrations with PBS-T. Membranes were then washed 5× over 30 min with PBS-T. Proteins were detected by enhanced chemiluminescence.

MTT viability assay

After treatment as indicated in the Figure Legends or Results, cell were incubated with 100 μL of 12 mM MTT (3-(4,5-dim-ethylthiazol-2-yl)-2,5-diphenyltetrazolium bromide) reagent for 4 h at 37°C, 10% CO_2. Next, 2 ml of dimethyl sulfoxide was added to solubilize the formazan and the plate was read at 570 nm in a spectrophotometer.

SMARTPOOL® siRNA mediated knockdown of Bcl-2

Stable NSC34 OGC cells were transfected with either the SMARTPOOL® (Thermo Scientific, Pittsburgh, PA, USA) siRNA against mouse Bcl-2 or non-target siRNA pool using the Dharama-FECT transfection protocol. Briefly, 25 nM of appropriate siRNA per well was incubated with 5 μL of DharmaFECT transfection reagent separately with serum-free medium for 5 min at ~25°C. siRNA and DharmaFECT in serum-free medium were mixed and incubated at ~25°C for 20 min. The mixture of siRNA/Dharama-FECT was then

added to the cells and incubated for 48 h at 37°C and at 10% CO_2 before subsequent experiments were completed.

Immunoprecipitation

Whole rat brain was obtained from two Sprague–Dawley P7 (post-natal day 7) rats and homogenized with eight passes of the loose pestle and four passes of the tight pestle from a Dounce homogenizer in 0.1% Triton X-100 in lysis buffer containing protease inhibitors and 10 mM reduced GSH. The immunoprecipitation reaction consisted of 200 μg of protein lysate with 4 μg antibody to Bcl-2, OGC, or non-immune IgG; reactions were incubated overnight at 4°C with mixing by inversion. Next, 100 μL of protein A/G agarose beads was incubated with the immunoprecipitation reactions for 4 h, 4°C, mixing by inversion. Samples were spun down and washed 3× with 0.1% Triton X-100 in lysis buffer, before being resolved by sodium dodecyl sulfate–polyacrylamide gel electrophoresis and immunoblotted. Total lysate was loaded at 100 μg of protein. All animal procedures were performed according to a protocol approved by the University of Denver Institutional Animal Care and Use Committee.

Statistical analysis

One-way ANOVA followed by a *post hoc* Tukey's test or an unpaired Student's *t*-test was performed to determine statistical significance between datasets. A $p < 0.05$ was considered statistically significant.

Results

Stable over-expression of OGC specifically increases the mitochondrial GSH pool

To establish the successful over-expression of V5-tagged OGC we used a parental (untransfected) NSC34 cell line to compare with two separate NSC34 cell lines which showed resistance to geneticin. We immunoblotted all cell lines for both the V5 epitope tag and OGC protein levels. Both stable OGC cell lines displayed abundant expression of V5 and OGC compared to parental NSC34 cells (indicated as wild type (WT) in Fig. 1a). Lysates were also blotted against β3 tubulin, a neuron-specific control, thus indicating that the over-expression of OGC did not appear to change the neuronal phenotype of the NSC34 cells. Interestingly, β3 tubulin expression was actually enhanced in the cell lines over-expressing OGC. Furthermore, blotting for another inner mitochondrial membrane GSH transporter, DIC, revealed no significant change in expression following stable over-expression of OGC. Finally, the cell lines were also immunoblotted for the rate-limiting enzyme in GSH synthesis, GCL (catalytic subunit) and the OGC stable cell lines showed marked induction of this enzyme (Fig. 1a). Actin is shown as a loading control. Stable OGC cell lines were continually monitored for maintenance of high V5-OGC expression throughout the course of the experiments.

To examine the effects of stable OGC expression on mitochondrial GSH levels, stable cell lines and WT NSC34 cells were fractionated into mitochondrial and cytosolic fractions and GSH levels were measured. Both stable OGC cell lines displayed a significant and specific approximate two-fold increase in mitochondrial GSH levels compared to WT NSC34 cells

(Fig. 1b). Mitochondrial GSH concentrations calculated as nmoles/mg of protein were as follows, for WT, 24.4 ± 3.4, OGC 3, 50.3 ± 8.1, OGC 6, 57.6 ± 14.7 (mean ± SEM, $n = 6$). In contrast, no statistically significant changes in cytosolic GSH content were observed when the stable OGC cell lines were compared to WT NSC34 cells (Fig. 1c). It is notable that although OGC over-expression did not significantly increase cytosolic GSH, there was a trend toward this effect (see Fig. 1c). A previous study demonstrated that increased Bcl-2 expression induces an nuclear factor kappa-light chain enhancer of activated B cells (NFκB)-dependent enhancement in transcription of the rate-limiting enzyme in GSH synthesis, GCL (Jang and Surh 2004). Consistent with these previous findings, we observed that the stable OGC cell lines displayed a marked increase in both Bcl-2 (see Fig. 5a discussed below) and GCL expression (Fig. 1a). Thus, the apparent increase in cytosolic GSH observed with stable OGC over-expression may represent an increase in overall GSH synthesis. The percentage of mitochondrial GSH compared to cytosolic GSH was in a range consistent with previous studies, where the mitochondrial GSH pool is between 5% and 30% of total cellular GSH (Lash 2006). For WT NSC34 cells, mitochondrial GSH comprised 4.6 ± 1.1%; while for OGC 3 mitochondrial GSH was 7.2 ± 3.1% and for OGC 6 mitochondrial GSH was 12.2 ± 5.6% of total cellular GSH (mean ± SEM, $n = 7$) (Fig. 1c). These data further support the purity of the cellular fractionations, along with the immunoblots against Cox-IV, a mitochondrial specific protein, and α-tubulin, a cytosolic marker (Fig. 1d).

The stable OGC NSC34 cell lines are resistant to oxidative stress induced by hydrogen peroxide

To determine if the stable OGC cell lines were more resistant than WT NSC34 cells to oxidative stress, the reactive intermediate hydrogen peroxide (H_2O_2) was used. Here, we employed two doses of H_2O_2, 500 μM or 1 mM, for a period of 24 h. In Fig. 2a, brightfield images indicate the distinct cell death induced at both doses of H_2O_2 in the WT NSC34 cell line, and the striking resistance of both OGC stable cell lines to this oxidative stressor. To quantify the differences in cell viability between the WT and stable OGC cell lines, an MTT assay was employed. MTT reduction is commonly assumed to occur exclusively in mitochondria; however, several studies have depicted significant extra-mitochondrial involvement in MTT reduction (Berridge and Tan 1993; Liu *et al.* 1997). Furthermore, the MTT assay is widely used to determine cell viability. The WT cells displayed a significant loss of cell viability compared to the untreated controls at both 500 μM and 1 mM H_2O_2 (Fig. 2b). However, neither stable OGC cell line showed any significant decrease in cell viability at either dose of H_2O_2 (Fig. 2b). Upon completion of these experiments, it became clear that both OGC stable cell lines proliferated at a much higher frequency compared to the WT NSC34 cells. While all cell lines were plated at one million cells per well, increased proliferation of the stable OGC cell lines induced a greater cell density compared to WT NSC34 cells. This is important, because increased cell density can lead to increased expression of pro-survival proteins, such as Bcl-2 and Bcl-X_L (Zimmermann *et al.* 2005). This led us to question the effect of high proliferation frequency of the stable OGC NSC34 cell lines on their resistance to oxidative stress. To address the above possibility, we employed three different plating densities and exposed cells to H_2O_2. The WT NSC34 cells showed significant loss of cell viability with treatment of H_2O_2 at each cell density tested (data not shown). In contrast, neither stable OGC cell line showed a significant decrement in

cell viability in response to H_2O_2 treatment at any of the densities (data not shown). These results indicate that the observed resistance of OGC cell lines to H_2O_2 is not because of enhanced proliferation or higher cell density.

Stable over-expression of OGC prevents loss of cell viability in the presence of ethacrynic acid

Ethacrynic acid has previously been shown to non-preferentially deplete both mitochondrial and cytosolic pools of GSH, and thus induce cell death. Therefore, to determine if enhanced mitochondrial GSH transport affords protection from this GSH depleting agent, we examined the toxic effects of ethacrynic acid. The WT NSC34 cell line displayed significantly reduced cell viability following exposure to two doses of ethacrynic acid (Fig. 2c). In contrast, stable OGC over-expression prevented this loss of cell viability induced by ethacrynic acid (Fig. 2c). Therefore, enhanced mitochondrial GSH transport is sufficient to prevent cell death induced by the depletion of both cytosolic and mitochondrial pools of GSH, illustrating the key role of the mitochondrial GSH pool in maintaining neuronal survival. A previous report demonstrated that ethacrynic acid treatment of NSC34 cells under similar conditions to those used in our experiment, significantly reduced both mitochondrial and cytosolic pools of GSH, with the mitochondrial pool being preferentially depleted at an earlier time point than the cytosolic pool (Muyderman *et al.* 2009). Analysis of GSH pools in the WT and OGC3 stable cell lines revealed that both cytosolic and mitochondrial GSH pools were reduced following exposure to ethacrynic acid. However, the mitochondrial GSH content in ethacrynic acid treated, OGC over-expressing cells was sustained above the level observed in mitochondria of untreated parental (WT) NSC34 cells (Table 1). On the other hand, OGC over-expression had no effect on the ethacrynic acid-induced reduction in the cytosolic GSH pool (Table 1). Similar data were obtained for the OGC6 stable cell line (data not shown). Thus, bolstering the mitochondrial GSH pool via OGC over-expression provides enough of an increase in the mitochondrial GSH pool to protect against an acute ethacrynic acid challenge.

Over-expression of OGC renders NSC34 cells resistant to nitrosative stress

The nitric oxide donor, sodium nitroprusside (SNP), was used to induce nitrosative stress and determine if enhanced mitochondrial GSH transport would protect from this insult. Brightfield images taken after SNP treatment indicated that the WT NSC34 cells were sensitive to both doses of SNP used, but no toxic effect was observed in either of the OGC stable cell lines (data not shown). The WT cells displayed a significant loss of cell viability as measured by an MTT assay at both SNP doses (Fig. 2d). However, neither OGC cell line showed any significant decrement in cell viability in response to SNP (Fig. 2d). Therefore, over-expression of the mitochondrial GSH transporter, OGC, and thus enhancement of mitochondrial GSH transport, reduces neuronal sensitivity to nitrosative stress conditions.

Stable over-expression of OGC does not protect NSC34 motor neuron-like cells from staurosporine-induced apoptosis

We next examined the ability of enhanced mitochondrial GSH transport, and thus increased mitochondrial GSH content, to protect from a non-oxidative cell death mechanism. Stable

OGC cell lines and WT NSC34 cells were treated with two doses of staurosporine (STS), a classically Bax-dependent method of inducing intrinsic apoptosis. WT and OGC 3 NSC34 cells both displayed a caspase 3-generated cleavage product of Poly-ADP ribose polymerase in response to STS treatment, indicating an apoptotic mode of cell death (Fig. 3a). Furthermore, WT NSC34 cells and both stable OGC cell lines displayed similar significant decreases in cell viability at both doses of STS (Fig. 3b). Therefore, stable over-expression of the mitochondrial GSH transporter, OGC, did not afford protection from this classical (non-oxidative) apoptotic insult. These data demonstrate the specificity of increased mitochondrial GSH transport for enhancing the resistance of neuronal cells to oxidative damage.

Chemical inhibition of OGC transport function specifically reduces mitochondrial GSH and resensitizes OGC stable cell lines to oxidative stress induced by hydrogen peroxide

Phenylsuccinate is a chemical analog of 2-oxoglutarate that specifically blocks transport through the OGC. To show that enhanced mitochondrial GSH transport was responsible for conferring resistance of both stable OGC cell lines to oxidative stress, phenylsuccinate was used to inhibit OGC-dependent transport. First, we examined the effects of phenylsuccinate on mitochondrial GSH levels. Both OGC stable cell lines showed significant and specific decreases in mitochondrial GSH suggesting that phenylsuccinate successfully reduced the transport of GSH into the mitochondria (Fig. 4a). Following phenylsuccinate treatment, the mitochondrial GSH concentrations calculated as nmoles/mg were 29.8 ± 5.3 for OGC 3 and 20.9 ± 5.5 for OGC 6 (mean ± SEM, $n = 3$). Therefore, phenylsuccinate lowered the mitochondrial GSH concentrations in both OGC 3 and OGC 6 to approximately WT levels (24.4 ± 3.4 nmoles/mg, as discussed above in Fig. 1). Cox-IV and GAPDH immunoblots indicate the purity of the mitochondrial fractions (Fig. 4a). Next, OGC stable cell lines were co-incubated with phenylsuccinate and H_2O_2, phenylsuccinate alone, or H_2O_2 alone and cell viability was measured. Following incubation with phenylsuccinate or H_2O_2 alone, neither OGC cell line showed any significant decrease in cell viability (Fig. 4b and c). However, both cell lines showed significant reductions in cell viability at both doses of H_2O_2 when OGC was simultaneously inhibited with phenylsuccinate, as compared to cells that were treated with H_2O_2 alone (Fig. 4b and c).

Specific increases in mitochondrial GSH induce an increase of the anti-apoptotic protein Bcl-2

Previous studies using recombinant proteins or transient over-expression constructs have shown that Bcl-2 and OGC are interacting partners (Gallo *et al.* 2011; Wilkins *et al.* 2012). Thus, Bcl-2 protein levels were examined in the OGC stable cell lines and interestingly, both cell lines displayed increased Bcl-2 expression, compared to WT NSC34 cells (Fig. 5a) (approximate 5-fold increase). To determine if the increased Bcl-2 expression was generally owing to stable OGC over-expression or more specifically, to increased mitochondrial GSH, WT NSC34 cells were chronically treated (for 48 h) with the cell-permeable GSH monoethylester (GSH-MEE). In Fig. 5b, we show that chronic exposure to GSH-MEE specifically increased mitochondrial GSH levels, with no significant effect on the cytosolic pool. Cox-IV and GAPDH immunoblots indicate the purity of the mitochondrial and cytosolic fractions (Fig. 5b). Next, WT NSC34 cells chronically treated with GSH-MEE

were immunoblotted for Bcl-2 protein levels, which were significantly increased compared to untreated WT NSC34 cells (Fig. 5c) (approximate 3-fold increase). Overall, these data show that an upregulation of Bcl-2 protein expression occurs as a result of specifically increased mitochondrial GSH levels.

The siRNA-mediated knockdown of Bcl-2 specifically decreases mitochondrial GSH and resensitizes OGC over-expressing NSC34 cells to oxidative stress

We have previously shown that inhibition of OGC-dependent GSH transport prevents the ability of Bcl-2 over-expression to protect Chinese hamster ovarian cells from H_2O_2-induced oxidative stress (Wilkins *et al.* 2012). Therefore, we hypothesized that Bcl-2 induction may be reciprocally necessary for OGC-dependent protection of NSC34 cells from oxidative stress. To determine if the increased expression of Bcl-2 was instrumental in rendering the OGC stable cell lines resistant to oxidative stress, we used a SMARTPOOL® siRNA to specifically knockdown Bcl-2 in the stable OGC 6 cell line. OGC 6 cells were transfected with either non-target or Bcl-2 siRNA for 48 h and Bcl-2 protein levels were examined. As shown in Fig. 6a, the Bcl-2 siRNA markedly reduced Bcl-2 protein levels compared to the non-target control (an average of 47.3 ± 8.1% reduction in Bcl-2 protein levels, mean ± SEM, $n = 6$). Next, we examined the effects of reduced Bcl-2 levels on mitochondrial GSH content. Knockdown of Bcl-2 protein levels induced a specific 35% reduction in mitochondrial GSH content compared to non-target transfected cells (Fig. 6b). Cox-IV and GAPDH blots indicate pure cellular fractionations (Fig. 6b). Based on the specific reduction in mitochondrial GSH with siRNA-mediated knockdown of Bcl-2 protein levels, we hypothesized that these cells would be resensitized to oxidative stress. Indeed, OGC 6 cells transfected with siRNA against Bcl-2 displayed a statistically significant reduction in cell viability with both concentrations of H_2O_2, whereas no decrease in cell viability was observed with the non-target control (Fig. 6c). Experiments were also completed comparing the non-target siRNA against a no transfection control and no significant differences in Bcl-2 protein levels, mitochondrial GSH content, or cell viability were observed (data not shown).

Bcl-2 and OGC co-immunoprecipitate from rat brain lysates in a GSH-dependent manner

As stated previously, Bcl-2 and OGC have been demonstrated to be interacting partners. However, past studies have used recombinant and protein over-expression systems to show the association between these two proteins (Gallo *et al.* 2011; Wilkins *et al.* 2012). Therefore, we aimed to determine if the Bcl-2 and OGC interaction could be observed in a system with endogenous levels of protein expression. Here, we used whole rat brain lysates in the presence of high (10 mM) GSH to perform co-immunoprecipitation reactions. As shown in Fig. 7a, Bcl-2 co-immunoprecipitated with OGC and OGC co-immunoprecipitated with Bcl-2 in a GSH-dependent manner. The co-immunoprecipitation did not occur without the addition of high GSH (Fig. 7b). Finally, an IgG immunoprecipitation is shown as a control for non-specific binding (Fig. 7a).

Discussion

Previous studies have shown that the over-expression of mitochondrial GSH transporters (OGC and DIC) renders kidney- and liver-derived cell lines resistant to apoptotic stimuli (Xu *et al.* 2006; Zhong *et al.* 2008). However, very limited information is available on the role of these mitochondrial GSH transporters in neuronal systems. Here, we generated stable V5-tagged OGC cell lines using immortalized mouse NSC34 motor neuron-like cells. NSC34 motor neuron-like cells afforded ease of transfection; however, because NSC34 cells are an immortalized cell line, they only approximate the phenotypic characteristics of motor neurons. NSC34 cells differ from primary motor neurons because they lack synaptic transmission; however, they do share some similarities with motor neurons such as, sensitivity to insults that block voltage-gated ion channels and axonal transmission (Durham *et al.* 1993). Furthermore, the stable NSC34 OGC cell lines appeared to retain their neuronal phenotype, as shown through the continued expression of neuron-specific β3 tubulin, despite showing enhanced proliferation compared to parental NSC34 cells. Stable over-expression of OGC in the NSC34 cells led to a significant and specific increase in mitochondrial GSH levels and a corresponding increase in resistance of these cells to oxidative stress. These data suggest an interesting question of whether OGC might play a role in mitochondrial GSH transport within primary motor neurons. Indeed, OGC is abundantly expressed in mouse spinal cord (M. Wilkins and A. Linseman, unpublished data). Thus, further studies are warranted in primary motor neurons, especially given the profound resistance observed with enhanced mitochondrial GSH transport against both oxidative and nitrosative stress, major pathogenic factors in neurodegenerative motor diseases like amyotrophic lateral sclerosis (ALS).

While it may be anticipated that over-expression of a mitochondrial GSH transporter would lead to an increase in mitochondrial GSH and enhanced neuronal cell resistance to oxidative and nitrosative stress, it is quite novel that stable OGC cells also displayed a marked increase in Bcl-2 protein levels. Furthermore, the up-regulation of Bcl-2 could be recapitulated by chronic exposure of parental NSC34 cells to a cell-permeable form of GSH, which similarly produced a specific increase in mitochondrial GSH levels. Our data are consistent with previous studies which showed that modulation of total cellular GSH levels results in the alteration of Bcl-2 protein levels (Celli *et al.* 1998; Ho *et al.* 1997). However, these prior studies only examined the relationship between manipulating total cellular GSH content and Bcl-2 protein expression. To our knowledge, this is the first study to demonstrate that Bcl-2 protein expression is explicitly regulated by mitochondrial GSH levels.

Several mechanisms could lead to an increase in Bcl-2 protein levels, including decreased proteasome-dependent degradation, de-repression of Bcl-2 transcription or translation (such as through microRNAs), or up-regulation of Bcl-2 transcription. Celli *et al.* (1998) showed that Bcl-2 protein levels were down-regulated in response to depletion of total cellular GSH levels in a liver cell line because of increased Bcl-2 protein degradation by the proteasome. MicroRNA involvement has also been implicated in the regulation of Bcl-2 expression. Two microRNAs, miR-15 and miR-16, have been shown to down-regulate Bcl-2 expression, a process that is deficient in chronic lymphocytic leukemia lymphocytes (Cimmino *et al.*

2005). Whether microRNAs are relevant to the up-regulation of Bcl-2, demonstrated here in our model is unknown; however, it is interesting to note that chronic lymphocytic leukemia lymphocytes have been shown to have an approximate two-fold increase in GSH, a common observation in most cancerous cells which over-express Bcl-2 (Ferraris *et al.* 1994).

While the above mechanisms may contribute to increased Bcl-2 protein levels in response to changes in total cellular GSH, mitochondrial redox alterations specifically have been shown to modulate protein kinase A (PKA) and downstream cyclic AMP response element binding protein (CREB) transcriptional activities (Ferraris *et al.* 1994; Ryu *et al.* 2005). Importantly, CREB has been shown to contribute significantly to Bcl-2 transcriptional regulation and is known as a redox sensitive transcription factor (Wilson *et al.* 1996). PKA is activated through an auto-phosphorylation event induced by cyclic AMP (cAMP), and a discrete pool of PKA appears to localize to the outer mitochondrial membrane where it is associated with A kinase anchoring protein (AKAP121) (Affaitati *et al.* 2003; Ginsberg *et al.* 2003). It has been previously shown that cAMP generated through a mitochondrial soluble adenylyl cyclase which is sensitive to ATP production allows for the phosphorylation and activation of mitochondrial localized PKA (Acin-Perez *et al.* 2009). Furthermore, antioxidants such as the iron chelator deferoxamine can increase the activity of mitochondrial PKA/CREB, while inhibition of PKA prevented the protective action of deferoxamine against GSH depletion (Ryu *et al.* 2005). Finally, the association of PKA with AKAP121 has been shown to promote the translocation of mRNA of nuclear-encoded mitochondrial proteins from the cytosol to the outer mitochondrial membrane, thus allowing their translation to occur locally at that site (Ginsberg *et al.* 2003). While we have not yet elucidated the mechanism allowing for the up-regulation of Bcl-2 protein levels in response to chronically elevated mitochondrial GSH, an increase in Bcl-2 transcription through the PKA/CREB axis, specifically at the level of the mitochondria, is most supported by previous studies. Overall, our data indicate a novel mitochondria-to-nucleus redox sensitive signaling mechanism in the regulation of Bcl-2 protein expression.

We have previously shown that Bcl-2 interacts with OGC in a GSH-dependent manner using both recombinant and protein over-expression systems (Wilkins *et al.* 2012). The Bcl-2 homolog, CED9, was also shown to be an interacting partner for the OGC homolog, MISC-1, in *C. elegans*, suggesting that this interaction is evolutionarily conserved (Gallo *et al.* 2011). Here, we show that Bcl-2 and OGC interact in a GSH-dependent manner in rat brain lysates, thus verifying this interaction within an endogenous expression system. We have previously demonstrated the dependence of the protective effects of Bcl-2 on the transport function of OGC; treatment of Chinese hamster ovarian cells over-expressing both Bcl-2 and OGC with the OGC inhibitor, phenylsuccinate, prevented the ability of Bcl-2 to protect from oxidative stress (Wilkins *et al.* 2012). Our current data show that the knockdown of Bcl-2 through siRNA prevents the ability of over-expressed OGC to protect NSC34 cells from oxidative stress. The knockdown of Bcl-2 also led to a significant and specific decrease in mitochondrial GSH levels in the stable OGC over-expressing cell lines. Therefore, we have provided compelling evidence that OGC and Bcl-2 are interacting partners that work in conjunction to modulate mitochondrial GSH transport and sensitivity to oxidative and nitrosative stress conditions. Moreover, the protection against oxidative

stress afforded by Bcl-2 or OGC over-expression is reciprocally dependent upon one another.

Overall, we show that enhancing mitochondrial GSH transport through the over-expression of OGC provides two main cytoprotective mechanisms. First, over-expression of OGC specifically increased mitochondrial GSH content and rendered NSC34 cells resistant to oxidative and nitrosative stress conditions. Second, the specific increase in mitochondrial GSH induced by the over-expression of OGC produced a corresponding increase in Bcl-2 protein levels. These findings are important to the field of neurodegeneration especially, because Bcl-2 expression is often decreased in these diseases. For example, Bcl-2 expression is diminished in spinal cord tissue from both ALS patients and in a mutant Cu/Zn Superoxide dismutase 1 (SOD1) mouse model of familial ALS (Mu *et al.* 1996; Vukosavic *et al.* 1999). Furthermore, it has been shown that the ratio of GSH/GSSG is also decreased in mitochondria isolated from spinal cord of mutant SOD1 mouse models of familial ALS, and we have recently found that total mitochondrial GSH content is significantly decreased in lumbar spinal cord from end-stage G93A mutant SOD1 mice (M. Wilkins and A. Linseman, unpublished data; Ferri *et al.* 2006). Therefore, modulating mitochondrial GSH transport could prove to be a significant therapeutic target in neurodegenerative diseases like ALS in which Bcl-2 expression is diminished.

Acknowledgments

This study was supported by a Merit Review grant from the Department of Veterans Affairs (to D.A.L.) and an R01 grant NS062766 from the National Institutes of Health (to D.A.L.).

Abbreviations used

AKAP121	A kinase anchoring protein
ALS	amyotrophiclateralsclerosis
CGN	cerebellar granule neuron
CHO	Chinese hamster ovarian cell
CNS	central nervous system
Cox-IV	cytochrome *c* oxidase or complex IV
CREB	cyclic AMP response element binding protein
DIC	*Slc25a10* dicarboxylate carrier
EA	ethacrynic acid
ETC	electron transport chain
GAPDH	glyceraldehyde 3-phosphate dehydrogenase
GSH	glutathione
GSH-MEE	glutathione monoethyl ester
IP	immunoprecipitation

MOS	mitochondrial oxidative stress
OGC	*Slc25a11* 2-oxoglutarate carrier
PKA	protein kinase A
PS	phenylsuccinate
ROS	reactive oxygen species
SNP	sodium nitroprusside
STS	staurosporine
TCC	*Slc25a1* tricarboxylate carrier
WT	wild type

References

Acin-Perez R, Salazar E, Kamenetsky M, Buck J, Levin LR, Manfredi G. Cyclic AMP produced inside mitochondria regulates oxidative phosphorylation. Cell Metab. 2009; 9:265–276. [PubMed: 19254571]

Affaitati A, Cardone L, de Cristofaro T, Carlucci A, Ginsberg MD, Varrone S, Gottesman ME, Avvedimento EV, Feliciello A. Essential role of A-kinase anchor protein 121 for cAMP signaling to mitochondria. J Biol Chem. 2003; 278:4286–4294. [PubMed: 12427737]

Berridge MV, Tan AS. Characterization of the cellular reduction of 3-(4,5-dimethylthiazol-2-yl)-2,5-diphenyltetrazolium bromide (MTT):subcellular localization, substrate dependence, and involvement of mitochondrial electron transport in MTT reduction. Arch Biochem Biophys. 1993; 303:474–482. [PubMed: 8390225]

Celli A, Que FG, Gores GJ, LaRusso NF. Glutathione depletion is associated with decreased Bcl-2 expression and increased apoptosis in cholangiocytes. Am J Physiol. 1998; 275:G749–G757. [PubMed: 9756506]

Cimmino A, Calin GA, Fabbri M, et al. miR-15 and miR-16 induce apoptosis by targeting BCL2. PNAS. 2005; 102:13944–13949. [PubMed: 16166262]

Durham HD, Dahrouge S, Cashman NR. Evaluation of the spinal cord neuron X neuroblastoma hybrid cell line NSC-34 as a model for neurotoxicity testing. Neurotoxicology. 1993; 14:387–395. [PubMed: 7909362]

Ferraris AM, Rolfo M, Mangerini R, Gaetani GF. Increased glutathione in chronic lymphocytic leukemia lymphocytes. Am J Hematol. 1994; 47:237–238. [PubMed: 7942792]

Ferri A, Cozzolino M, Crosio C, Nencini M, Casciati A, Gralla EB, Rotilio G, Valentine JS, Carrì MT. Familial ALS-superoxide dismutases associate with mitochondria and shift their redox potentials. PNAS. 2006; 103:13860–13865. [PubMed: 16945901]

Filomeni G, Rotilio G, Ciriolo MR. Cell signalling and the glutathione redox system. Biochem Pharmacol. 2002; 64:1057–1064. [PubMed: 12213605]

Gallo M, Park D, Luciani DS, Kida K, Palmieri F, Blacque OE, Johnson JD, Riddle DL. MISC-1/OGC links mitochondrial metabolism, apoptosis, and insulin secretion. PLoS ONE. 2011; 6:e17827. [PubMed: 21448454]

Ginsberg MD, Feliciello A, Jones JK, Avvedimento EV, Gottesman ME. PKA-dependent Binding of mRNA to the Mitochondrial AKAP121 Protein. J Mol Biol. 2003; 327:885–897. [PubMed: 12654270]

Ho YS, Lee HM, Mou TC, Wang YJ, Lin JK. Suppression of nitric oxide-induced apoptosis by N-acetyl-L-cysteine through modulation of glutathione, bcl-2, and bax protein levels. Mol Carcinog. 1997; 19:101–113. [PubMed: 9210957]

Jang JH, Surh YJ. Bcl-2 attenuation of oxidative cell death is associated with up-regulation of gamma-glutamylcysteine ligase via constitutive NF-kappaB activation. J Biol Chem. 2004; 279:38779–38786. [PubMed: 15208316]

Kamga CK, Zhang SX, Wang Y. Dicarboxylate carrier-mediated glutathione transport is essential for reactive oxygen species homeostasis and normal respiration in rat brain mitochondria. Am J Physiol Cell Physiol. 2010; 299:C497–C505. [PubMed: 20538765]

Kann O, Kovács R. Mitochondria and neuronal activity. Am J Physiol Cell Physiol. 2007; 292:C641–C657. [PubMed: 17092996]

Lash LH. Mitochondrial glutathione transport: physiological, pathological and toxicological implications. Chem Biol Interact. 2006; 163:54–67. [PubMed: 16600197]

Lin MT, Beal MF. Mitochondrial dysfunction and oxidative stress in neurodegenerative diseases. Nature. 2006; 443:787–795. [PubMed: 17051205]

Linseman DA, Laessig T, Meintzer MK, McClure M, Barth H, Aktories K, Heidenreich KA. An essential role for Rac/Cdc42 GTPases in cerebellar granule neuron survival. J Biol Chem. 2001; 276:39123–39131. [PubMed: 11509562]

Liu Y, Peterson DA, Kimura H, Schubert D. Mechanism of cellular 3-(4,5-Dimethylthiazol-2-yl)-2,5-diphenyltetrazolium bromide (MTT) reduction. J Neurochem. 1997; 69:581–593. [PubMed: 9231715]

Meredith MJ, Reed DJ. Status of the mitochondrial pool of glutathione in the isolated hepatocyte. J Biol Chem. 1982; 257:3747–3753. [PubMed: 7061508]

Meredith MJ, Reed DJ. Depletion in vitro of mitochondrial glutathione in rat hepatocytes and enhancement of lipid peroxidation by adriamycin and 1,3-bis(2-chloroethyl)-1-nitrosourea (BCNU). Biochem Pharmacol. 1983; 32:1383–1388. [PubMed: 6860357]

Mu X, He J, Anderson DW, Trojanowski JQ, Springer JE. Altered expression of bcl-2 and bax mRNA in amyotrophic lateral sclerosis spinal cord motor neurons. Ann Neurol. 1996; 40:379–386. [PubMed: 8797527]

Muyderman H, Wadey AL, Nilsson M, Sims NR. Mitochondrial glutathione protects against cell death induced by oxidative stress and nitrative stress in astrocytes. J Neurochem. 2007; 102:1369–1382. [PubMed: 17484727]

Muyderman H, Hutson PG, Matusica D, Rogers ML, Rush RA. The human G93A-superoxide dismutase-1 mutation, mitochondrial glutathione and apoptotic cell death. Neurochem Res. 2009; 34:1847–1856. [PubMed: 19399611]

Ryu H, Lee J, Impey S, Ratan RR, Ferrante RJ. Antioxidants modulate mitochondrial PKA and increase CREB binding to D-loop DNA of the mitochondrial genome in neurons. PNAS. 2005; 102:13915–13920. [PubMed: 16169904]

Schafer FQ, Buettner GR. Redox environment of the cell as viewed through the redox state of the glutathione disulfide/glutathione couple. Free Radic Biol Med. 2001; 30:1191–1212. [PubMed: 11368918]

Silver I, Erecinska M. Oxygen and ion concentrations in normoxic and hypoxic brain cells. Adv Exp Med Biol. 1998; 454:7–16. [PubMed: 9889871]

Vukosavic S, Dubois-Dauphin M, Romero N, Przedborski S. Bax and Bcl-2 interaction in a transgenic mouse model of familial amyotrophic lateral sclerosis. J Neurochem. 1999; 73:2460–2468. [PubMed: 10582606]

Wadey AL, Muyderman H, Kwek PT, Sims NR. Mitochondrial glutathione uptake: characterization in isolated rat brain mitochondria and astrocytes in culture. J Neurochem. 2009; 109:101–108. [PubMed: 19393015]

Wilkins HM, Marquardt K, Lash LH, Linseman DA. Bcl-2 is a novel interacting partner for the 2-oxoglutarate carrier and a key regulator of mitochondrial glutathione. Free Radic Biol Med. 2012; 52:410–419. [PubMed: 22115789]

Wilkins HM, Kirchhof D, Manning E, Joseph JW, Linseman DA. Mitochondrial glutathione transport is a key determinant of neuronal susceptibility to oxidative and nitrosative stress. J Biol Chem. 2013; 288:5091–5101. [PubMed: 23283974]

Wilson BE, Mochon E, Boxer LM. Induction of bcl-2 expression by phosphorylated CREB proteins during B-cell activation and rescue from apoptosis. Mol Cell Biol. 1996; 16:5546–5556. [PubMed: 8816467]

Xu F, Putt DA, Matherly LH, Lash LH. Modulation of expression of rat mitochondrial 2-oxoglutarate carrier in NRK-52E cells alters mitochondrial transport and accumulation of glutathione and susceptibility to chemically induced apoptosis. J Pharmacol Exp Ther. 2006; 316:1175–1186. [PubMed: 16291728]

Zhong Q, Putt DA, Xu F, Lash LH. Hepatic mitochondrial transport of glutathione: studies in isolated rat liver mitochondria and H4iie rat hepatoma cells. Arch Biochem Biophys. 2008; 474:119–127. [PubMed: 18374655]

Zimmermann AK, Loucks FA, Le SS, Butts BD, Florez-McClure ML, Bouchard RJ, Heidenreich KA, Linseman DA. Distinct mechanisms of neuronal apoptosis are triggered by antagonism of Bcl-2/Bcl-X(L) versus induction of the BH3-only protein Bim. J Neurochem. 2005; 94:22–36. [PubMed: 15953346]

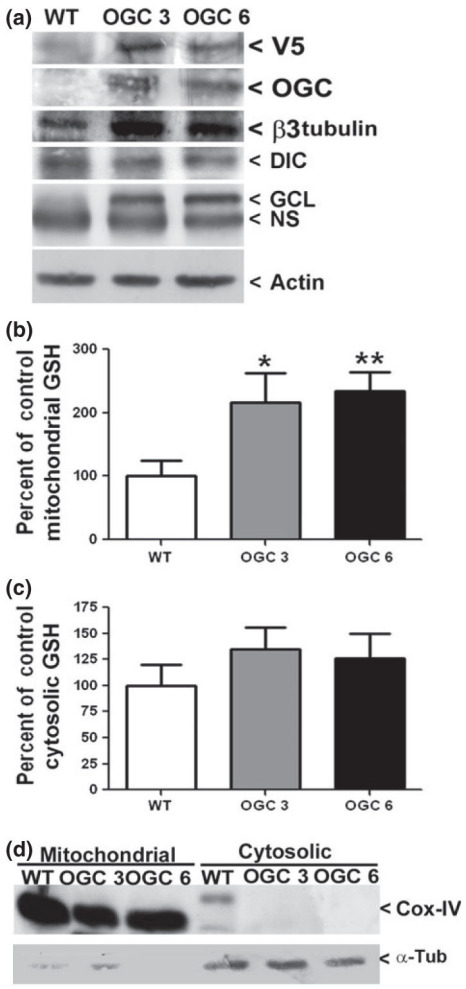

Fig. 1.

Stable over-expression of OGC specifically increases the mitochondrial glutathione (GSH) pool. (a) Whole cell lysates were resolved by sodium dodecyl sulfate–polyacrylamide gel electrophoresis (SDS–PAGE) and immunoblotted against V5, OGC, neuron-specific β3 tubulin, DIC, γ-glutamylcysteine ligase (GCL) catalytic subunit, and actin. OGC stable cell lines are indicated as OGC 3 and OGC 6; parental NSC34 cells are indicated as wild type (WT). NS, non-specific band. (b) Cells were fractionated by differential centrifugation and total mitochondrial GSH content was then measured using a DTNB colorimetric assay. Data are represented as a percentage of WT GSH measurements. *$p < 0.05$ versus WT mitochondrial GSH; **$p < 0.01$ versus WT mitochondrial GSH in an unpaired Student's *t*-test, $n = 7$, error bars indicate SE. (c) Cells were fractionated by differential centrifugation and total cytosolic GSH content was then measured using a DTNB colorimetric assay. Data are represented as a percentage of WT cytosolic GSH measurements. $n = 7$, error bars indicate SE. (d) Cellular fractions were resolved using SDS–PAGE and immunoblotted against Cox-IV and α-tubulin (α-Tub).

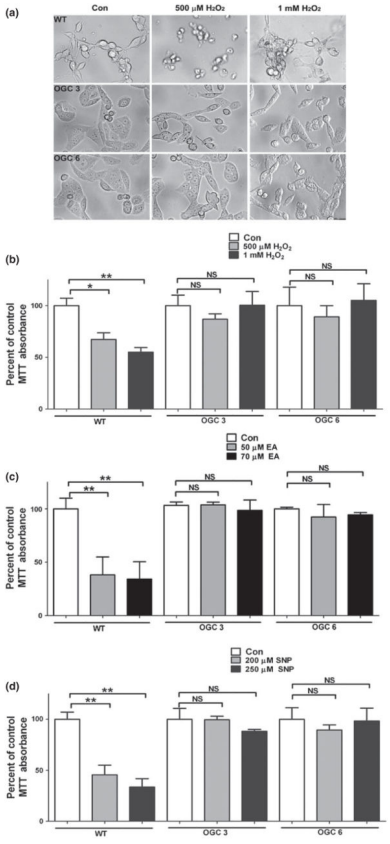

Fig. 2.

The stable OGC NSC34 cell lines are resistant to toxicity induced by hydrogen peroxide, ethacrynic acid, and sodium nitroprusside. (a) After plating cells at one million cells per well, cells were treated the following day with either vehicle control (Con); 500 μM H_2O_2 or 1 mM H_2O_2 overnight. Brightfield images were captured following treatment. (b) Cells were plated and treated as in (a), after which an 3-(4,5-dimethylthiazol-2-yl)-2,5-diphenyltetrazolium bromide (MTT) cell viability assay was completed. Data are represented as percent of Con for each cell line. *$p < 0.05$ versus wild-type (WT) Con; **$p < 0.01$, compared to WT Con; NS, not significant via a one-way ANOVA with *post hoc* Tukey's test, $n = 6$, error bars indicate SE. (c) Cells were treated as in (a), but with 50 μM or 70 μM ethacrynic acid (EA) instead of H_2O_2, following which an MTT cell viability assay was completed. Data are represented as a percent of Con for each cell line. **$p < 0.01$ compared to WT Con; NS, not significant via a one-way ANOVA with *post hoc* Tukey's test, $n = 4$, error bars indicate SE. (d) Cells were treated as in A, but with 200 μM or 250 μM sodium nitroprusside (SNP) instead of H_2O_2, following which an MTT cell viability assay was completed. Data are represented as a percent of Con for each cell line. **$p < 0.01$ compared to WT Con; NS, not significant via a one-way ANOVA with *post hoc* Tukey's test, $n = 4$, error bars indicate SE.

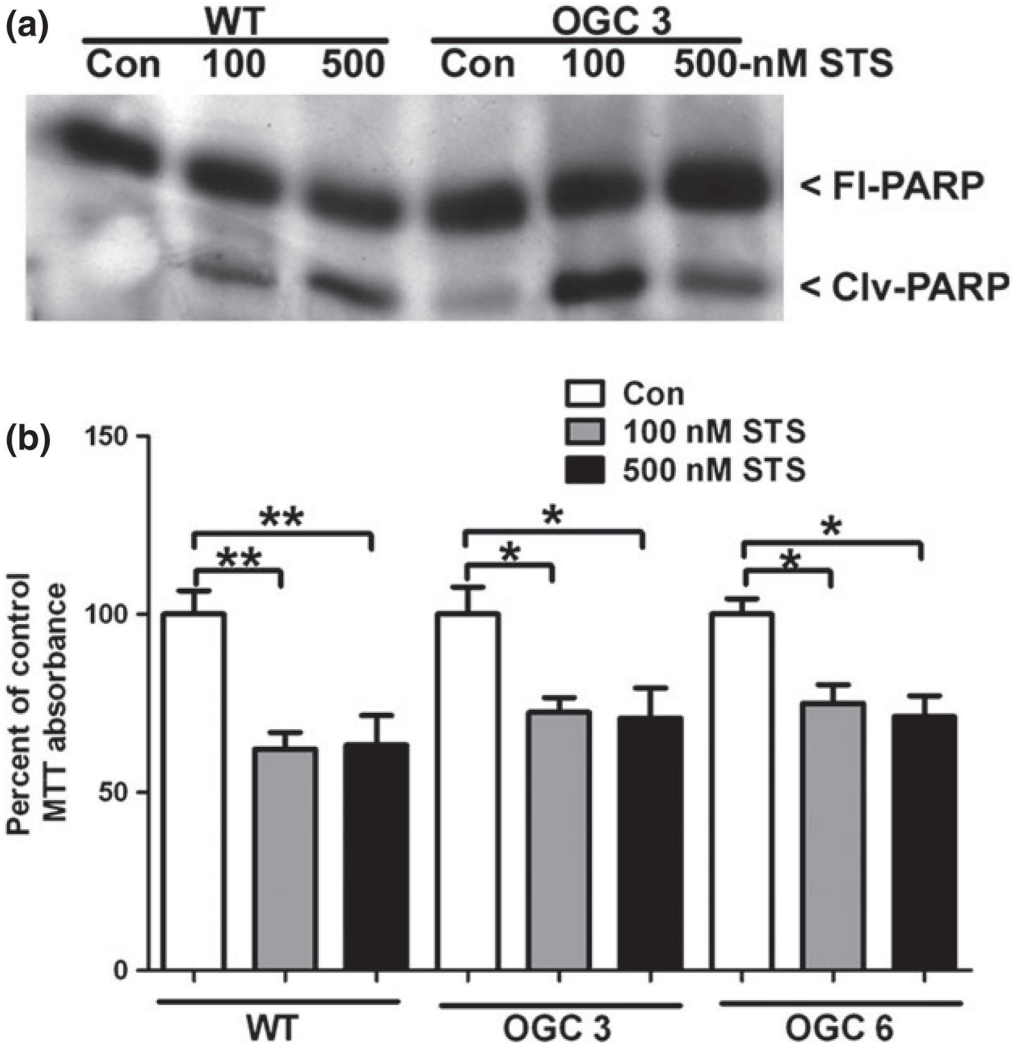

Fig. 3.

Stable over-expression of OGC does not protect NSC34 motor neuron-like cells from staurosporine-induced apoptosis. (a) Cells were plated at one million cells per well, following which cells were treated with vehicle control (Con); 100 nM or 500 nM staurosporine (STS) for 24 h. Cells were lysed and proteins were resolved by sodium dodecyl sulfate–polyacrylamide gel electrophoresis (SDS–PAGE), immunoblot against Poly-ADP ribose polymerase (PARP) was completed. FlPARP-full-length PARP, Clvg-PARP-cleavage of PARP. (b) Cells were treated as in (a), following which an 3-(4,5-dimethylthiazol-2-yl)-2,5-diphenyltetrazoli-um bromide (MTT) cell viability assay was completed, Data are represented as a percent of Con for each cell line. $^{**}p < 0.01$ compared to wild-type (WT) Con; $^{*}p < 0.05$ compared to OGC 3 or OGC 6 Con via a one-way ANOVA with *post hoc* Tukey's test, $n = 4$, error bars indicate SE.

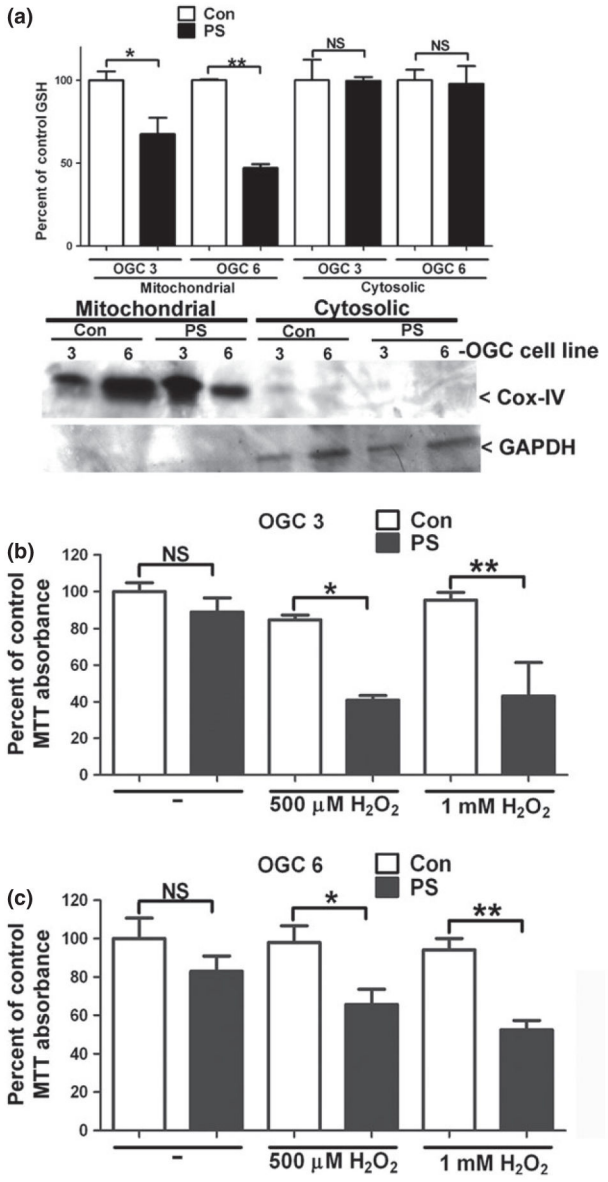

Fig. 4.

Chemical inhibition of OGC transport function specifically reduces mitochondrial glutathione (GSH) and resensitizes OGC stable cell lines to oxidative stress induced by hydrogen peroxide. (a) Stable OGC NSC34 cells were treated with 10 mM phenylsuccinate (PS) overnight. Cells were then fractionated using differential centrifugation. Cell fractions were measured for total GSH using a DTNB colorimetric assay. Data are represented as a percent of untreated control (Con) GSH. *$p < 0.05$ compared to OGC 3 Con **$p < 0.01$ versus OGC 6 Con; NS, not significant via a Student's *t*-test. $n = 4$, error bars indicated SE. Cell fractions were resolved by sodium dodecyl sulfate–polyacrylamide gel electrophoresis (SDS–PAGE) and immunoblotted against cytochrome *c* oxidase or complex IV (Cox-IV) and glyceraldehyde 3-phosphate dehydrogenase (GAPDH). (b) Stable OGC 3 NSC34 cells were treated with 10 mM PS alone or in combination with 500 μM or 1 mM H_2O_2. At 24 h

after treatment an 3-(4,5-dimethylthiazol-2-yl)-2,5-diphenyltetrazolium bromide (MTT) assay was completed and data are represented as percent of there presentative Con (i.e., the same treatment in the absence of PS). *$p < 0.05$, **$p < 0.01$ versus Con, NS, not significant; via a one-way ANOVA with *post hoc* Tukey's test $n = 3$, error bars indicate SE. (c) Stable OGC 6 NSC34 cells were treated with 10 mM PS alone or in combination with 500 μM or 1 mMH_2O_2. At 24 h after treatment an MTT assay was completed and data are represented as percent of the representative control Con (i.e., the same treatment in the absence of PS). *$p < 0.05$, **$p < 0.01$ versus Con, NS, not significant; via a one-way ANOVA with *post hoc* Tukey's test $n = 5$, error bars indicate SE.

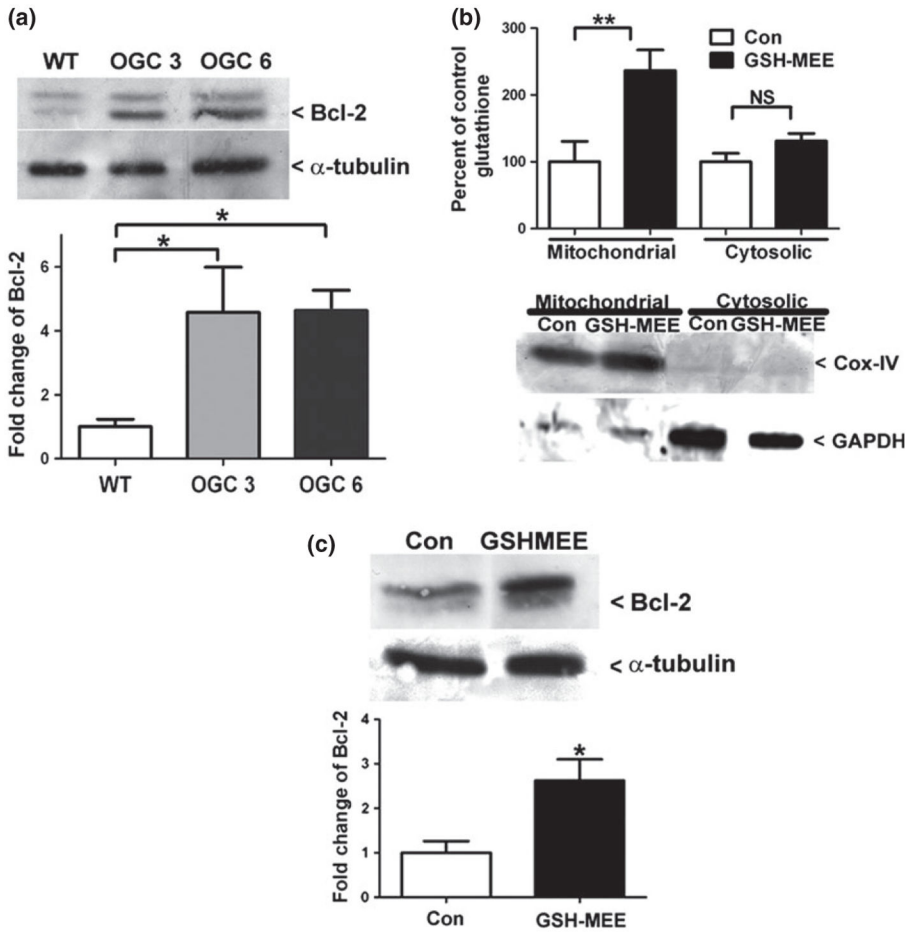

Fig. 5.

Specific increases in mitochondrial glutathione (GSH) induces an increase of the anti-apoptotic protein Bcl-2. (a) Lysates were resolved by sodium dodecyl sulfate–polyacrylamide gel electrophoresis (SDS–PAGE) and immunoblotted against Bcl-2 and α-tubulin. Densitometry was completed for Bcl-2 and was normalized to α-tubulin. Data are represented as percent of wild-type (WT) Bcl-2 levels. *$p < 0.05$ versus WT via a one-way ANOVA with *post hoc* Tukey's test, $n = 3$, error bars indicate SE. (b) WT NSC34 cells were treated for 48 h with 2 mM GSH-monoethyl ester (MEE), fractionated by differential centrifugation and total GSH was measured using a DTNB colorimetric assay. Data are represented as a percent of Con GSH. **$p < 0.01$ versus Con via an unpaired Student's *t*-test $n = 7$, error bar indicates SE. Samples were resolved by SDS–PAGE and immunoblotted against cytochrome *c* oxidase or complex IV (Cox-IV) and glyceraldehyde 3-phosphate dehydrogenase (GAPDH). (c) WT NSC34 cells treated as in (b) were lysed and proteins were resolved by SDS–PAGE. Immunoblots against Bcl-2 and α-tubulin were completed. Densitometry was completed for Bcl-2 and normalized to α-tubulin. Data are represented as a percent of the Con Bcl-2 expression. *$p < 0.05$ versus Con via an unpaired Student's *t*-test; $n = 3$, error bar indicates SE.

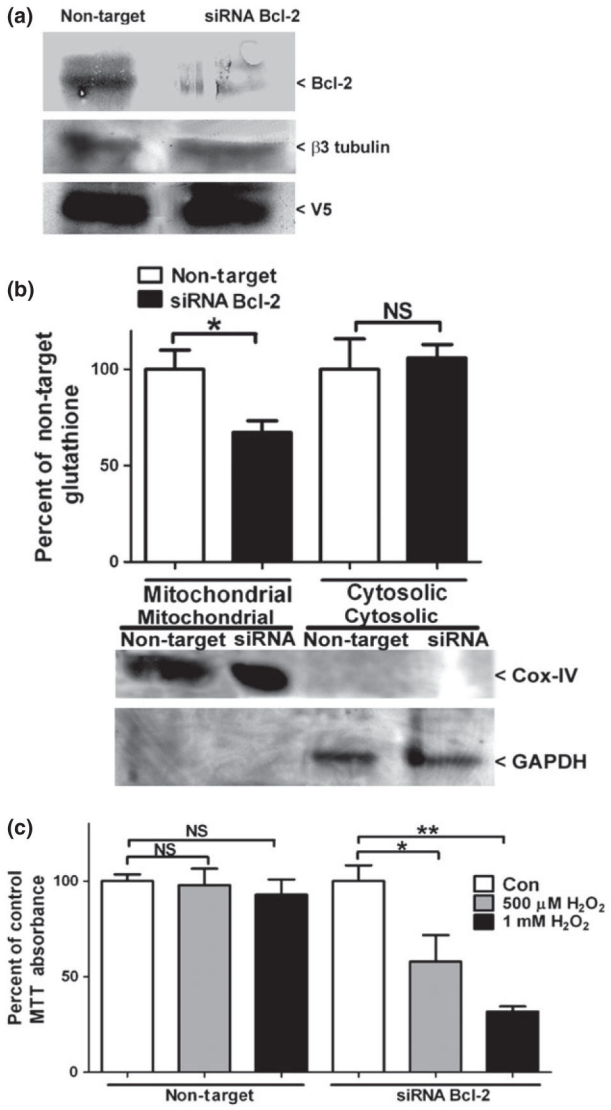

Fig. 6.

The siRNA-mediated knockdown of Bcl-2 specifically decreases mitochondrial glutathione (GSH) and resensitizes OGC over-expressing NSC34 cells to oxidative stress. (a) Stable OGC 6 NSC34 cells were transfected with either non-target or Bcl-2 siRNA at 25 nM for 48 h. Cells were lysed, proteins were resolved by sodium dodecyl sulfate–polyacrylamide gel electrophoresis (SDS–PAGE), and immunoblotted against Bcl-2, V5, and β3-tubulin. Densitometry of Bcl-2 normalized to β3 tubulin showed a 43.3 ± 8.1% (mean ± SEM, $n = 5$) reduction in Bcl-2 levels in siRNA Bcl-2-transfected cells compared to non-target transfection. (b) Cells transfected as in (a), then fractionated by differential centrifugation and total GSH content was measured using a colorimetric DTNB assay. Data are represented as a percent of the non-target control. *$p < 0.05$ compared to non-target via an unpaired Student's *t*-test, $n = 6$, error bars indicate SE. (c) Cells were transfected as in (a) treated with vehicle control (Con); 500 μM or 1 mM H_2O_2. Cell viability was assed via an 3-(4,5-dimethylthiazol-2-yl)-2,5-diphenyltetrazolium bromide (MTT) assay. *$p < 0.05$ versus Con

siRNA; **$p < 0.01$ versus Con siRNA; NS, not significant via a one-way ANOVA with *post hoc* Tukey's test. $n = 5$, error bars indicate SE.

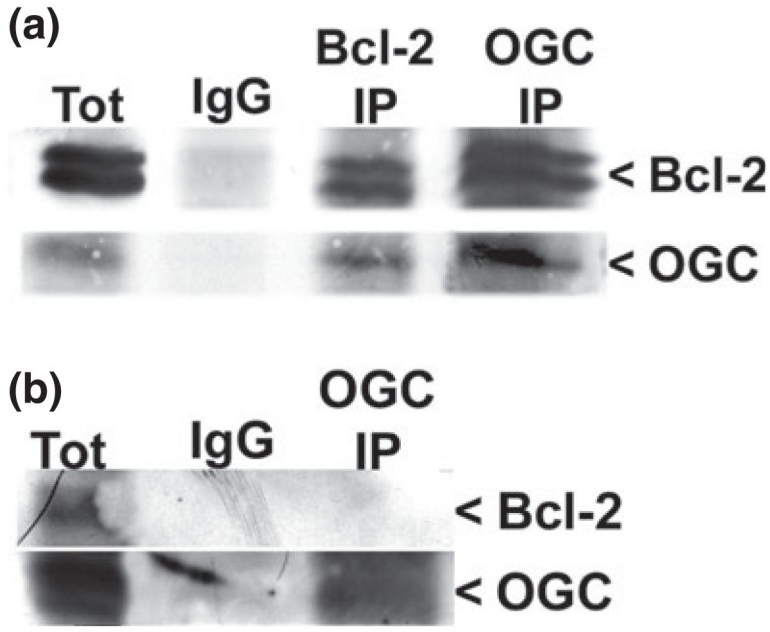

Fig. 7.

Bcl-2 and OGC co-immunoprecipitate from rat brain lysates in a glutathione (GSH)-dependent manner. (a) Whole rat brain was homogenized in 0.1% Triton X-100 in lysis buffer with protease inhibitors and 10 mM reduced GSH. Immunoprecipitation reactions were completed using either an IgG, Bcl-2, or OGC antibody. Samples were resolved by sodium dodecyl sulfate–polyacrylamide gel electrophoresis (SDS–PAGE) and immunoblotted against Bcl-2 and OGC. (b) Samples were prepared as in (a) except without GSH. Immunoprecipitation reactions were completed using either an IgG or OGC antibody. Samples were resolved by SDS–PAGE and immunoblotted against Bcl-2 and OGC. Tot, total lysate.

Table 1

GSH levels in response to ethacrynic acid treatment (% of WT Control)

Mitochondrial GSH	
WT control	100 ± 8
WT ethacrynic acid	72 ± 1
OGC3 control	199 ± 7
OGC3 ethacrynic acid	149 ± 20
Cytosolic GSH	
WT control	100 ± 7
WT ethacrynic acid	79 ± 3
OGC3 control	109 ± 11
OGC3 ethacrynic acid	77 ± 9

All values are mean ± SEM (n = 3 independent experiments).